DISTRIBUTION STATEMENT A. Approved for public release; distribution is unlimited.

Satellite SAR Exploitation and Imaging and Measurement of Oceanic Phenomena

Hans C. Graber
CSTARS - University of Miami
11811 SW 168th Street
Miami, FL 33177-, USA
phone: (305) 421-4952, fax: (305) 252-4407, email: hgraber@rsmas.miami.edu

William M. Drennan
Rosenstiel School of Marine and Atmospheric Science
University of Miami
4600 Rickenbacker Causeway
Miami, Florida 33149-1098
phone: (305) 421-4798, fax: (305) 421-4701, email: wdrennan@rsmas.miami.edu

Roland Romeiser
Rosenstiel School of Marine and Atmospheric Science
University of Miami
4600 Rickenbacker Causeway
Miami, Florida 33149-1098
phone: (305) 421-4645, fax: (305) 421-4701, email: rromeiser@miami.edu

Neil J. Williams
Rosenstiel School of Marine and Atmospheric Science
University of Miami
4600 Rickenbacker Causeway
Miami, Florida 33149-1098
phone: (305) 421-4656, fax: (305) 421-4701, email: nwilliams@rsmas.miami.edu

Michael F. Caruso
CSTARS - University of Miami
11811 SW 168th Street, Miami, FL 33177-, USA
phone: (305) 421-4973, fax: (305) 252-4407, email: mcaruso@rsmas.miami.edu

Award #: N00014-09-1-0392

LONG-TERM GOALS

This proposal consisted of six individual, but interelated projects. A common component of all tasks was the exploitation of satellite imagery. The six projects are listed as the following tasks:

Task 1: Air-Sea Interactions in Typhoon Conditions

Report Documentation Page

Form Approved
OMB No. 0704-0188

1. REPORT DATE **30 SEP 2014**	2. REPORT TYPE	3. DATES COVERED **00-00-2014 to 00-00-2014**

4. TITLE AND SUBTITLE **Satellite SAR Exploitation and Imaging and Measurement of Oceanic Phenomena**	5a. CONTRACT NUMBER 5b. GRANT NUMBER 5c. PROGRAM ELEMENT NUMBER
6. AUTHOR(S)	5d. PROJECT NUMBER 5e. TASK NUMBER 5f. WORK UNIT NUMBER
7. PERFORMING ORGANIZATION NAME(S) AND ADDRESS(ES) **University of Miami,Rosenstiel School of Marine and Atmospheric Science,4600 Rickenbacker Causeway,Miami,FL,33149**	8. PERFORMING ORGANIZATION REPORT NUMBER
9. SPONSORING/MONITORING AGENCY NAME(S) AND ADDRESS(ES)	10. SPONSOR/MONITOR'S ACRONYM(S) 11. SPONSOR/MONITOR'S REPORT NUMBER(S)

12. DISTRIBUTION/AVAILABILITY STATEMENT
Approved for public release; distribution unlimited

13. SUPPLEMENTARY NOTES

14. ABSTRACT

15. SUBJECT TERMS

16. SECURITY CLASSIFICATION OF:			17. LIMITATION OF ABSTRACT	18. NUMBER OF PAGES	19a. NAME OF RESPONSIBLE PERSON
a. REPORT **unclassified**	b. ABSTRACT **unclassified**	c. THIS PAGE **unclassified**	**Same as Report (SAR)**	**10**	

Task 2: Satellite Observations of Surface Signatures and Properties of Internal Waves in Straits

Task 3: Satellite Observations, Surface Signature and Properties of Nonlinear Internal Waves

Task 4: Satellite Observations of Surface Signatures in the Philippine Sea

Task 5: Satellite Observations of Oceanographic Processes for Quantifying, Predicting, and Exploiting Uncertainty (QPE)

Task 6: Exploitation of Commercial Satellite Radars

The long term goal of this project was to employ satellite SAR imagery to the quantitative analysis of typhoons, internal waves, ocean surface features, sea state prediction and coastal dynamics. To achieve this, a variety of satellite SAR sensors with different imaging frequencies, multi-polarizations and different beam modes were used to determine which combination of the above capabilities could provide the best solution.

OBJECTIVES

For simplicity we provide only a primary objective of each task.

a) **Task 1:** To determine the characteristics of typhoons with satellite SAR imagery.

b) **Task 2:** To complement the acquisition and analysis of conventional radar intensity images and other data by direct high-resolution imaging of surface current fields from space by along-track InSAR.

c) **Task 3:** To measure surface signatures and Bragg modulations during the passage of soliton packets.

d) **Task 4:** To improve the characterizations of the Philippine Archipelago Straits dynamics we propose to acquire satellite data, in particular synthetic aperture radar (SAR) imagery of features and processes present in these straits.

e) **Task 5:** To determine the structure, the seasonal and annual variability of the cold dome over the outer continental shelf northeast of Taiwan and the position and variability of the Kuroshio Current, in particular excursions onto the continental shelf.

f) **Task 6:** To explore innovative uses for commercial radar applications.

APPROACH

Satellite based Synthetic Aperture Radar (SAR) can operate day and night and in all weather condition. This is of importance especially in the Southeast Asia region where most of the time there is a persistent cloud cover and optical sensors such as MODIS to image internal waves are not frequently useful. However, radars penetrate clouds which ultimately are useful in typhoons. Furthermore, radars are truly sensing the surface and therefore observe the impact of the atmosphere on the ocean surface. SAR can provide large spatial coverage up to 500 km wide swaths using the ScanSAR mode but at lower resolution (~50 to 100 m) for the directional wave spectra, surface wind vectors, and surface roughness. The high-resolution of SAR wind retrievals make these data suitable for understanding

tropical cyclone morphology. In particular, the wind structure of eye wall replacement and the formation of thunderstorms and tornados in hurricanes can be imaged from all-weather SARs.

SAR imaging of internal waves provides the necessary geospatial context in terms of internal wave (IW) characteristics such as number of solitons, wave and crest length, refraction and shoaling, and origins. These images were also used to guide ship and glider operations in areas where IWs were present.

Task 1: From July to October 2010 a field experiment was carried out east of Taiwan in the primary region with high probability of typhoon tracks (Figure 1a). As part of the experiment we deployed two pairs of EASI (Extreme Air-Sea Interaction) and ASIS (Air-Sea Interaction Spar) buoys (Figure 1b) in international waters about 200 km apart. The buoys were equipped with extensive meteorological and oceanographic instrumentation to provide detailed measurements of the fluxes and properties of the air-sea interface.

We also utilized two remote sensing techniques which consisted of satellite-based imagery from RadarSat-2, TerraSar-X, Envisat ASAR, Cosmo-SkyMed and ERS-2; and a ship-borne marine X-band system (WaMoS) on the R/V Revelle. Figure 2 shows a summary of the quicklook images collected during Typhoon Megi. Using multiple satellite systems allowed for a good coverage of the storm after entering the experimental domain and across the Philippines and even into the Taiwan Straits. The synthetic aperture radar (SAR) images are especially valuable in determining the eye location and characteristics of storms. The radar backscatter data is used to derive wind speed and direction. Similarly the radar data can be used to estimate wave heights and wave directions. The marine radar systems on ships can also derive wind speed and direction, directional wave properties including spectra from is grazing angle observations. The range of measurements from ship radar is more limited and extends to about 3 nm.

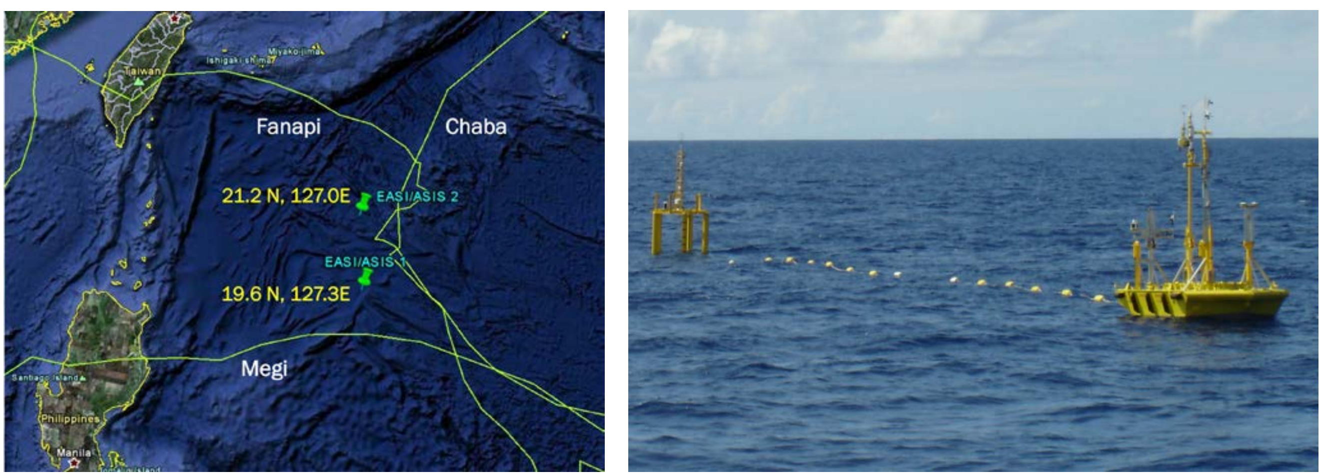

Figure 1: a) Deployment locations of the EASI/ASIS buoys in the Western Pacific with tracks of three of the typhoons passing by during the 2010 typhoon season. b) Deployed EASI/ASIS buoys in the Western Pacific.

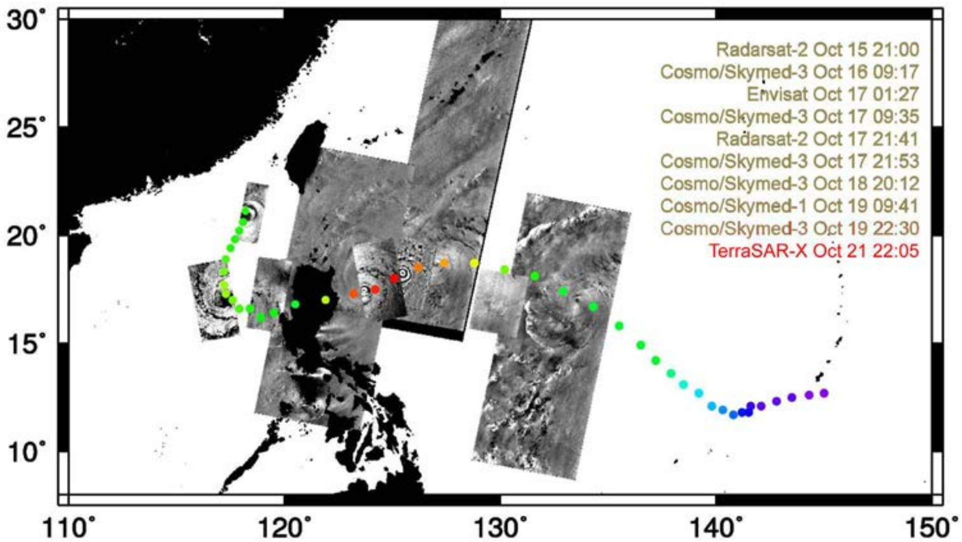

Figure 2: Multi satellite radar collections along the track of Typhoon Megi.

Task 2 and Task 3: Marine radars operate by transmitting and receiving pulses of microwaves that interact with the rough sea surface. The radar echo from the sea surface is primarily dependent on small-scale ripple waves due to Bragg scattering. IWs are accompanied by a spatially and temporally varying surface current field. Marine radars show IWs as adjacent bands of weak and strong backscatter that propagate with the IW packet's velocity. As for SAR images, such features can either result from hydrodynamic interactions between the short surface waves and the horizontal surface currents caused by IWs, or from surfactants that accumulate in IW flow convergence zones and dampen the short surface waves there.

A novel method called the Radon Transform (RT) was applied to retrieve IW information from marine radar data. First, the images were divided by their respective radar backscatter ramps to produce near-homogeneous intensities. The ramp-corrected images were then used to retrieve IW packet speed and direction, employing a combination of Radon Transform and cross-correlation techniques. In a next step, the images were geo-referenced and corrected for the IW packet motion. By averaging a 4 minute sequence of such preprocessed radar images, we can now significantly enhance the IW signatures. The resulting IW-enhanced images are fed into our IW signature retrieval algorithm, where we used localized Radon Transform techniques to trace the signatures of each individual soliton, yielding IW soliton maps. From such maps, one can easily extract parameters such as wavelength, velocity, and curvature for each IW soliton.

Figure 3 (left) shows a transect through a polar X-band radar image of an IW-enhanced image with its IW peaks and troughs marked by black and red dashed lines, respectively. An iterative approach that is based on a localized Radon Transform technique is applied to track each soliton, starting from the peaks found within the transect. A zoom into our IW-enhanced image with the retrieved IW signatures as well as the position of the transect are shown in Figure 3 (right).

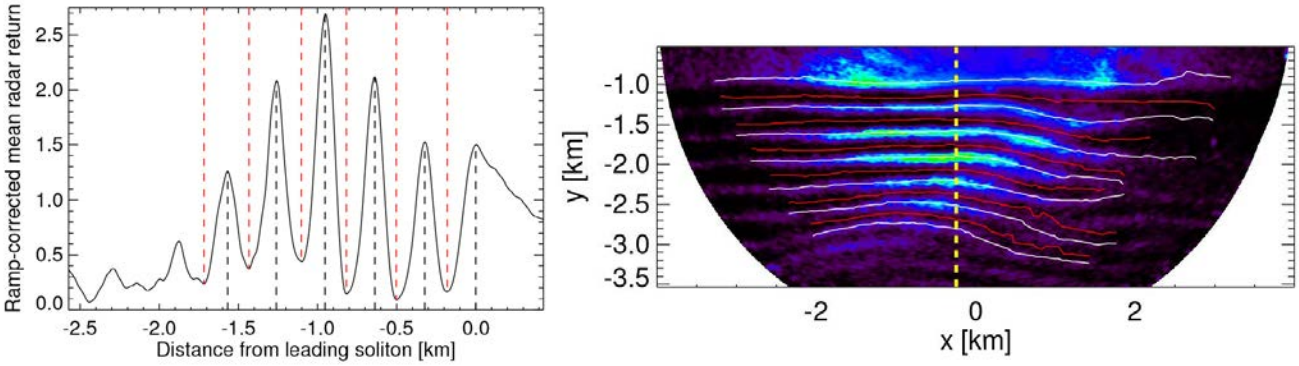

Figure 3: Transect with IW peaks and troughs marked by dashed lines (left) and corresponding image with the transect position marked by a yellow dashed line and the detected IW signatures marked by white and red solid lines (right).

Task 4: The Philippine Archipelago is known to generate strong gap jets blowing through the valley of its volcanic mountains. ENVISAT synthetic aperture radar (SAR) images during the 2004–2009 winter monsoon seasons (November–March) were analyzed using the wind field algorithm derived in Task 1. The wind fields revealed the presence of strong jets emanating from the mountain gaps in the lee of the Philippine Archipelago. Jet characteristics exhibited similar features of classical jets in water bodies. The Philippine Island gap winds were compared to those from theoretical literature and experimental studies. For all jets, the initial jet width dictated the distance at which a jet became self-similar, wherein a larger initial jet width required a greater distance for self-similarity. Figure 4 shows examples of gap jet wind fields derived from the SAR backscatter data. The jet features, long streaks emanating out of the valleys are quite obvious in contrast to the low wind speeds in the shadow (lee) of the mountain peaks.

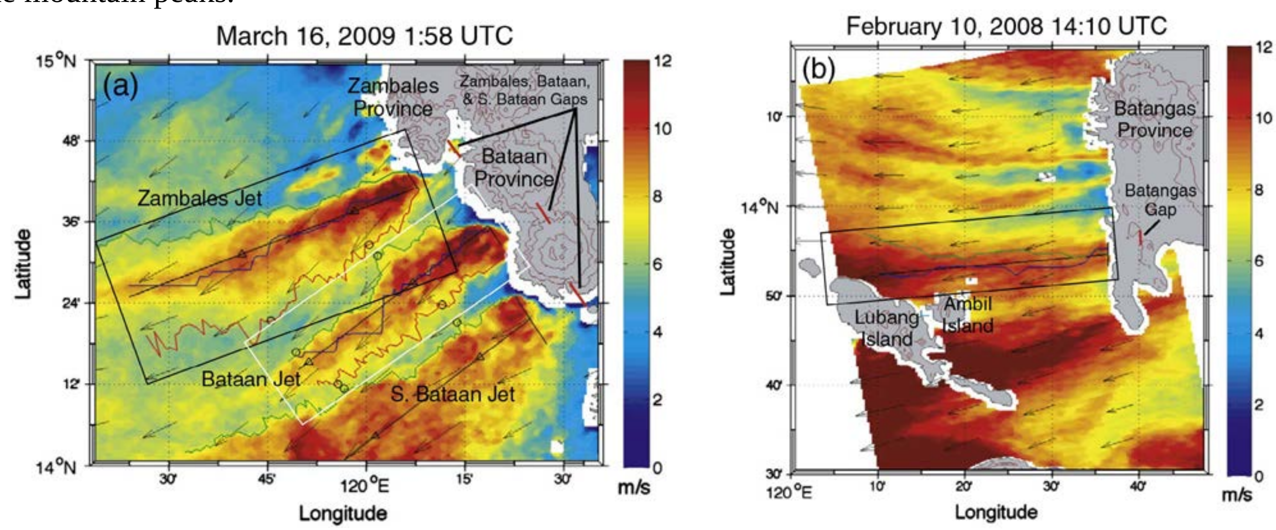

Figure 4: Examples of (a) classic (black box) and decreasing (white box) jet cases on March 16, 2009 1:58 UTC and (b) increasing jet case on February 10, 2008 14:10 UTC. The background is SAR-derived wind speed (m/s), with vectors denoting SAR-derived wind direction. Rectangular boxes denote the jets of interest. The green line denotes jet half-width (km), the perpendicular black line represents initial jet width (d, km), the straight black line is the jet centerline, and the blue line represents wind speed maxima (m/s) coordinates associated with the Principal Component Analysis technique from which the jet centerline is fit. Here d=6 km for (a) and d=5 for (b).

Task 5: The Ocean northeast of Taiwan has a large continental shelf, complex slope bathymetry, an upwelling region, a variable coastal current, a strong boundary current and abundant internal waves. Intense fishing activity inhibits comprehensive mooring measurements. These features make it difficult to understand the physical processes of this region. In support of the main field program for the QPE DRI in August/September 2009, 15 long strips of SAR images were acquired over the continental shelf northeast of Taiwan and the Kuroshio Current east of Taiwan. The collection focused on ascending and descending passes for ERS-2 and TerraSAR-X data using different beam modes that would include ScanSAR, standard and fine beam modes depending on the location. Similarly we collected MODIS SST images and other EO sensors that have infra-red channels such as ASTER (Advanced Spaceborne Thermal Emission and Reflection Radiometer), a high resolution imaging instrument flying on Terra.

Figure 5 shows a TerraSAR-X image over the northeast Taiwan shelf with abundant internal waves and soliton interaction patterns. Non-linear internal waves are observed in the satellite imagery and are used to deduce propagation patterns. The internal waves in this region are characterized by elaborate wave patterns created by multiple internal wave propagation directions and intersection angles. Although the images acquired show complicated internal wave patterns, three preferred pathways were found to exist. The first is offshore to the southeast toward deep water. The second is northwest toward the coast of China similar to internal wave patterns observed in other shelf regions. The third is orthogonal to the first two, propagating to the northeast along the shelf break. This third pathway produces the complex patterns frequently observed in satellite imagery of the region.

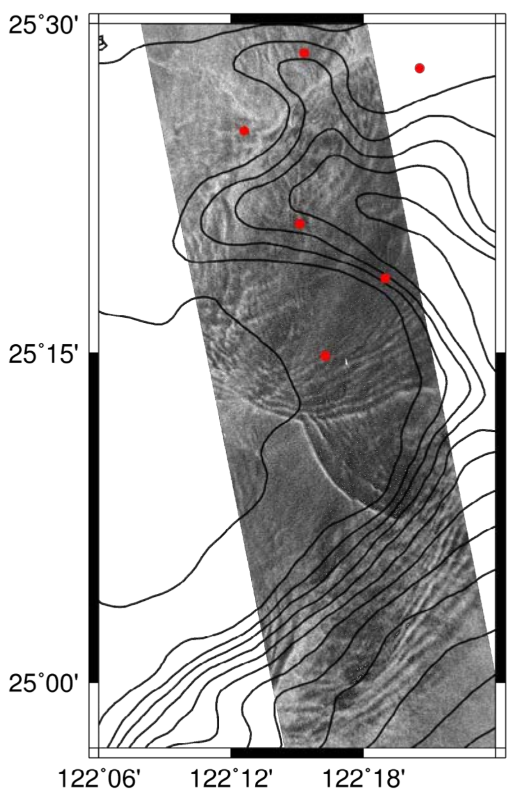

Figure 5: A TerraSAR-X image collected on 9 August 2009 showing interacting internal wave patterns and soliton groups propagating in multiple directions.

The majority of internal waves along the shelfbreak are classic depression waves generated by the internal tide along the shelfbreak. The remaining internal wave signatures are possibly generated by the encroachment of the Kuroshio Current on the shelf or the persistent cold dome. Additional internal waves may be trans-basin waves advecting onto the shelf from the Ilan Ridge or may be remnants of interacting wave packets (Figure 6). From the analysis of the imagery we found 220 internal wave (IW) packets with more than 2,407 waves (cf. Figure 6). There are clearly some hotspots of persistent internal waves located on the shelf and over the entrance to the canyons.

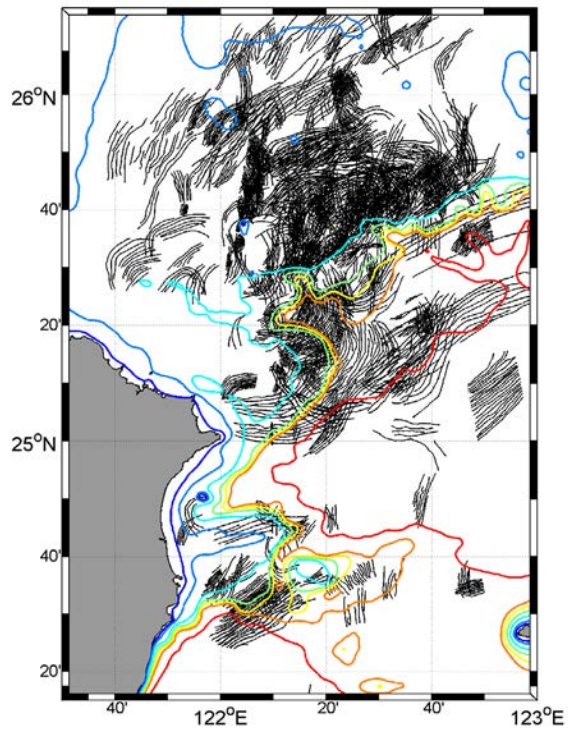

Figure 6: Locations of internal wave fronts identified from SAR imagery acquired between 2007 and 2010 from ERS-2 and TerraSAR-X.

The histogram of propagation directions (Figure 7) shows the primary pathways are generally oriented perpendicular to the bathymetry. The majority of the internal wave packets are traveling southeast (90° - 150°) toward the open ocean. The secondary propagation direction is to the northeast (270° - 330°) toward the coast. This propagation direction is frequently seen along the shelf in the South China Sea and the New York/Mid Atlantic Bight. A tertiary pathway exists towards the northeast (30° - 90°) along the shelf break. Note that the range of propagation directions along shore and offshore results in a peak in the histogram at the arbitrary delineation of 90° toward the east.

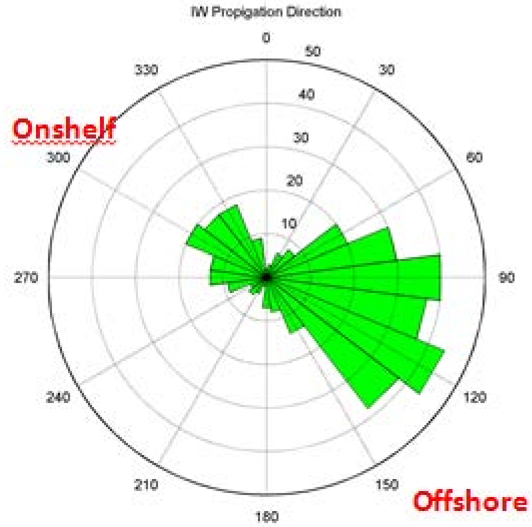

Figure 7: The propagation direction of internal waves from historical data. The northwest or onshore direction and southeast or offshore directions are dominant. However, internal waves also travel to the southwest toward the east coast of Taiwan. Internal waves also propagate toward the northeast along the shelfbreak.

RESULTS

This projects generated 13 peer-reviewed publications and 4 more in review as well as 5 conference proceedings. In addition the project supported four graduate students of which three received their PhDs and one more will finish in May 2015. The project also supported two post-doctoral scholars.

Below is a list of doctoral thesis and journal article publications loosely associated with each task. We also include the abstract for each publication.

DOCTORAL THESIS

Björn Lund, October 2012, Principal Advisor, (**RSMAS**). Thesis: *Currents from X-Band Marine Radar Measurements of Internal Waves*

Henry Potter, March 2014, Committee Member, (**RSMAS**). Thesis: *A Study of Turbulent Processes at the Air-Sea Interface in High Wind Speeds*

Clarence O. Collins, III, August 2014, Principal Advisor, (**RSMAS**). Thesis: *Typhoon Generated Surface Gravity Waves Measured by Nomad-Type Buoys*

Astrid Werkmeister, expected May 2015, Principal Advisor, (**RSMAS**). *Thesis: Vertical Structure and Wind-Wave Interaction in the Boundary Layer of Tropical Cyclones Derived from SAR Imagery*

PUBLICATIONS

Task 1:

D'Asaro, E.A., P.G. Black, L.R. Centurioni, Y.-T. Chang, S.S. Chen, R. Foster, **H.C. Graber**, P. Harr, V. Hormann, R.-C. Lien, I.-I. Lin, T.B. Sanford, T.-Y. Tang, and C.-C. Wu, 2013: Impact of typhoons on the ocean in the pacific: ITOP. *Bull. Americ. Meteo. Soc*., **95**(9), 1405–1418. doi: http://dx.doi.org/10.1175/BAMS-D-12-00104.1

Drennan, W.M., **H.C. Graber**, C.O. Collins III, A. Herrera, H. Potter, R.J. Ramos, and N.J. Williams, 2014: EASI: An air-sea interaction buoy for high winds. *J. Atmos. Oceanic Technol*., **31**, 1397-1409. DOI: 10.1175/JTECH-D-13-00201.1

Romeiser, R., **H.C. Graber**, M.J. Caruso, R.E. Jensen, D.T. Walker, A.T. Cox, 2014: A New Approach to Ocean Wave Parameter Estimates From C-Band ScanSAR Images. *IEEE Trans. Geosci. Remote Sens.*, **53**(3), 1320 – 1345.

Collins III, C.O., B. Lund, R.J. Ramos, W.M. Drennan, **H.C. Graber**, 2014: Wave Measurement Intercomparison and Platform Evaluation during the ITOP (2010) Experiment. *J. Atmos. Oceanic Technol.*, **31**, 2309–2329. doi: http://dx.doi.org/10.1175/JTECH-D-13-00149.1

Collins, C.O., B. Lund, T. Waseda, and **H.C. Graber**, 2014: On recording sea surface elevation with accelerometer buoys: lessons from ITOP (2010). *Ocean Dynam.*, **64**(6), 895-904.

Lund, B., C.O. Collins, **H.C. Graber**, E. Terrill, and T.H.C. Herbers, 2014: Marine radar ocean wave retrieval's dependency on range and azimuth. *Ocean Dynam.*, **64**(7), 999-1018.

Potter, H., C.O. Collins III, R.J. Ramos, N.J. Williams, W.M. Drennan, **H.C. Graber**, 2014: In situ measurements of momentum fluxes in typhoons. *J. Atmos. Sci*., doi: 10.1175/JAS-D-14-0025.1

Tamura, H., W.M. Drennan, E. Sahlee, **H.C. Graber**, 2014: Spectral form and source balance of short gravity waves. *J. Geophys. Res.,* In press.

Werkmeister, A.A. and **H.C. Graber**, 2014: Wind induced inertial currents measured by a drifting buoy. In review: *J. Geophys. Res.*

Horstmann, J., S. Falchetti, C. Wackerman, S. Maresca, M. Caruso and **H.C. Graber**, 2014: High Resolution Tropical Cyclone Winds Retrieved from Satellite Borne C-band Cross Polarized Synthetic Aperture Radar. *IEEE Trans. Geosci. Remote Sens.*, In review.

Task 2 and 3:

Lund, B., **H.C. Graber**, J. Xue, and R. Romeiser, 2012: Analysis of internal wave signatures in marine radar data. *IEEE Trans. Geosci. Remote Sens*. **51**(9), 4840-4852.

Lund, B., J. Xue, R. Romeiser, and **H.C. Graber**, 2012: Retrieval of internal wave signatures from marine radar data. *IGARSS 2012*, München, Germany, 22-27 July 2012.

Lund, B., **H.C. Graber**, R. Romeiser, 2012: Wind retrieval from shipborne nautical X-band radar data. *IEEE Trans. Geosci. Remote Sens*., **50**(10), 3800 – 3811.

Lund, B., **H.C. Graber**, J. Horstmann, and E. Terrill, 2012: Ocean surface wind retrieval from stationary and moving platform marine radar data. *IGARSS 2012*, München, Germany, 22-27 July 2012.

Lund, B., C.O. Collins III, H.C. Graber, E. Terrill, 2013: On the Imaging of Surface Gravity Waves by Marine Radar: Implications for a Moving Platform. *13th Int. Workshop on Wave Hindcasting and Forecasting & 4th Coastal Hazard Symposium*. Banff, AB, Canada.

Lund, B., **H.C. Graber**, K. Hessner, and N.J. Williams, 2015: On shipboard marine X-band radar near-surface current “calibration”. Submitted to *J. Atmos. Oceanic Technol*.

Task 4:

Gierach, M.M., **H.C. Graber**, M.J.Caruso, 2012: SAR-derived gap jet characteristics in the lee of the Philippine Archipelago. *Rem. Sens. Environ.,* **117**, 289-300. (doi:10.1016/j.rse.2011.10.004)

Task 5:

Duda, T.F., A.E. Newhall, G. Gawarkiewicz, M.J. Caruso, **H.C. Graber**, Y.-J. Yang, J. Sen, 2012: Significant internal waves and internal tides at a shelf edge and canyon region northeast of Taiwan. *J. Mar. Res.* (Special Issue), **71**(1-2), 47-81.

Caruso, M.J., R. Ramos, **H.C. Graber**, 2014: Internal wave propagation pathways off northeast Taiwan. *IEEE Trans. Geosci. Remote Sens.,* in preparation.

Alford, M.H., T. Peacock, M.C. Buijsman, L.R. Centuroni, S.-Y. Chao, M.-H. Chang, D.M. Farmer, O.B. Fringer, K.-H. Fu, P. Gallacher, **H.C. Graber**, K.R. Helfrich, S. Jachec, C. Jackson, Jody M. Klymak, Dong S. Ko, Sen Jan, T. M. Shaun Johnston, Sonya Legg, I-Huan Lee, Ren-Chieh Lien, Jennifer A. MacKinnon, Matthieu J. Mercier, Jim N. Moum, Ruth Musgrave, Jonathan D. Nash, Theresa Paluszkiewicz, Jae-Hun Park, Andrew I. Pickering, Robert Pinkel, Luc R. Rainville, Steven Ramp, Daniel R. Rudnick, Sutanu Sarkar, Alberto Scotti, Harper L. Simmons, Louis C. St. Laurent, Karan Venayagamoorthy, Yu-Huai Wang, Y. J. Yang, T. Y. Tang, 2014: The Formation and Fate of Internal Waves in the South China Sea. In review: *Nature*.

Task 6:

Romeiser, R., J. Horstmann, and **H.C. Graber**, 2010: A new scalloping filter algorithm for ScanSAR images. IGARSS 2010, Honolulu, 25-30 July 2010.

Romeiser, R., J. Horstmann, M.J. Caruso, and **H.C. Graber**, 2013: A descalloping post-processor for ScanSAR images of ocean scenes. *IEEE Trans. Geosci. Remote Sens.*, **51**(6), 3259-3272.